Photolysis Dynamics of Cyclopropyl and Oxiranyl Aryl Ketones: Drastic Ring-Activation Effect of Oxygen

Hahkjoon Kim, Taeg Gyum Kim, Joeoong Hahn, and Du-Jeon Jang*,†

School of Chemistry and Molecular Engineering, Seoul National University, Seoul 151-742, Korea

Dong Jo Chang and Bong Ser Park*

Department of Chemistry, Dongguk University, Seoul 100-715, Korea

Received: November 6, 2000; In Final Form: January 25, 2001

Although 1-(*o*-tolyl)-1-benzoylcyclopropane (**I**) and 2-(*o*-tolyl)-2-benzoyloxirane (**II**) are structurally analogous, they go through dramatically different reaction pathways upon absorption of photons. **I** yields a single photoproduct, while $^2H_2$-substituted **II** gives birth to three different photoproducts. The structural and kinetic features of the entire reaction intermediates have been measured with laser flash techniques. **I** at T_1 undergoes intramolecular hydrogen transfer at 2.3×10^8 s^{-1} from the methyl group to the carbonyl group to form a biradical intermediate, which transforms into a cyclized photoproduct (Φ 0.14; 5×10^7 s^{-1}). However, the carbonyl group of **II** at T_1 can abstract a hydrogen atom from the oxiranyl ring (6×10^7 s^{-1}) as well as from the methyl group (2.3×10^8 s^{-1}). The biradical intermediate from the former process immediately rearranges into a photoproduct (Φ 0.025), while the one from the latter transforms into a new oxiranyl ring-opened intermediate (1.1×10^8 s^{-1}) or a cyclized photoproduct (Φ 0.075; 3.3×10^8 s^{-1}). The new intermediate rearranges into another photoproduct (Φ 0.025; 3.7×10^7 s^{-1}). The dramatic changes of **II** are theoretically attributed to the drastic increase in the acidity and instability of the three-membered ring with oxygen substitution.

Introduction

Photochemistry of ketones containing a three-membered ring such as a cyclopropane or an oxirane adjacent to a carbonyl group has been extensively studied for over three decades.[1−14] Photochemical properties of these ketones are differentiated from those of isolated ketones without such rings. These are attributed to the conjugative nature between the rings and the carbonyl group. Even though many examples have been reported, most studies have been focused on product analysis with classical steady-state kinetics, and the detailed analyses on reaction dynamics have been lacking. Getting the complete pictures of the reaction mechanism with more direct kinetic measurements would be certainly helpful in understanding and predicting the photochemical behaviors of compounds containing such naturally abundant functional groups.

Among several types of photochemical processes available to cyclopropyl and oxiranyl ketones, ring-opening has been most frequently encountered. For example, *trans*-1,2-dibenzoylcyclopropane and *trans*-1-benzoyl-2-phenylcyclopropane photoisomerize via cyclopropyl ring rupture to yield *cis*-1,2-dibenzoylcyclopropane and *cis*-1-benzoyl-2-phenylcyclopropane, respectively.[15−18] Also, 1-benzoyl-2-methyl-2-phenyloxirane photorearranges into 1,3-diphenyl-3-buten-2-ol-1-one with oxiranyl ring-opening during the reaction pathway.[19] The ring-opening reaction can occur either directly in the excited reactants or in radical intermediates formed from the hydrogen-abstraction reaction of the excited carbonyl group, as illustrated with the above examples. Key reactions of the radical intermediates are the rearrangements of cyclopropylcarbinyl and oxiranylcarbinyl radicals. Kinetic studies of the rearrangements are vital to understand and predict their reaction pathways. The rate constants of the radical rearrangements have been indirectly determined with competition-kinetic methods in most cases. The rate constant for the ring-opening of the cyclopropylcarbinyl radical is about 10^8 s^{-1} at ambient temperature,[20] and that of the corresponding oxiranyl radical is at least 2 orders of magnitude faster than this.[21−23] Recently, more direct methods such as laser flash photolysis have been applied to measure rate constants for fast radical reactions.[24,25] All of these studies utilize the radical reactions that start from the required precursors of the corresponding radicals. Molecules should contain proper chromophores to be probed with laser flash photolysis.

In the course of our studies on the photochemistry of α-(*o*-tolyl)acetophenones with a small ring conjugated with the carbonyl group, we have envisioned that the photochemical reaction routes of these molecules could provide useful kinetic information on cyclopropylcarbinyl and oxiranylcarbinyl radical rearrangements.[26] Here we would like to describe mechanistic dichotomy between 1-(*o*-tolyl)-1-benzoylcyclopropane (**I**) and 2-(*o*-tolyl)-2-benzoyloxirane (**II**), which enables us to compare the ring-opening rates of cyclopropylcarbinyl and oxiranylcarbinyl radicals. The spectral and kinetic features of the intermediates occurring during their photolysis reactions in cyclohexane, as well as the photoproduct analyses, have been studied with laser flash photolysis methods. The product formation kinetics of **II** is compared with that of 2-phenyl-2-benzoyloxirane (**III**) as well, to understand the roles of the methyl group during the reaction. We have also carried out

* Authors to whom correspondence should be addressed.
† Telephone: +82−2−875−6624. Fax: +82−2−889−1568. E-mail: djjang@plaza.snu.ac.kr.

10.1021/jp004061v CCC: $20.00
Published on Web 03/15/2001

semiempirical calculations to explain the mechanistic dichotomy of the two molecular systems.

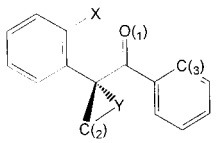

I: X = $C_{(1)}H_3$, Y = CH_2

II: X = $C_{(1)}H_3$, Y = O

III: X = H, Y = O

Experimental Section

Preparation of I. α-Methylidenyl-α-(*o*-tolyl)acetophenone was obtained with 85% yield by alpha methylenating α-(*o*-tolyl)-acetophenone with the aldol condensation using potassium carbonate and paraformaldehyde.[27] The resulting α,*β*-unsaturated ketone was treated with a mixture of NaH and trimethylsulfoxonium iodide in DMSO until all of the starting materials disappeared.[28] After regular workup and column chromatography using *n*-hexane and diethyl ether (30:1) as eluents, we obtained colorless liquid of **I** with 76% yield. ^{1}H NMR($CDCl_3$) δ 7.62−6.97(m, 9H), 2.14(s, 3H), 1.86(m, 2H), 1.33(m, 2H); ^{13}C NMR($CDCl_3$) δ 202.7, 139.9, 139.8, 138.7, 132.0, 131.0, 129.7, 129.2, 128.2, 127.8, 126.5, 35.7, 20.3, 18.6; IR(CCl_4) 3072, 3025, 1665 cm^{-1}; EI MS 236(M^+, 2.7), 208(10.4), 131-(16.5), 105(100), 77(47.7).

Preparation of II. α-Methylidenyl α-(*o*-tolyl)acetophenone, described in the preparation of **I**, was added to a mixture of 30% hydrogen peroxide solution in methanol and 6 M NaOH. The mixed solution was refluxed for 3 h. After regular workup and column chromatography using *n*-hexane and ethyl acetate (20:1) as eluents, colorless liquid was obtained with 94% yield. ^{1}H NMR($CDCl_3$) δ 8.10(distorted d, 2H, J = 7.5 Hz), 7.63−7.01(m, 7H), 3.43(d, 1H, J = 5.8 Hz), 3.19(d, 1H, J = 5.8 Hz), 2.37(s, 3H); ^{13}C NMR($CDCl_3$) δ 196.6, 138.3, 135.5, 135.0, 133.7, 131.1, 129.9, 129.3, 128.9, 128.3, 126.5, 64.4, 53.3, 20.3; IR(CCl_4) 3067, 2925, 1690, 1678 cm^{-1}; EI MS 238(M^+, 4.9), 133(90.1), 105(100), 77(66.3).

Preparation of $^2H_2$-Substituted II (II(d_2)). The synthetic procedures were the same as those of **II** except that paraformaldehyde-d_6 was used instead. ^{1}H NMR($CDCl_3$) δ 8.10(distorted d, 2H, J = 7.5 Hz), 7.63−7.01(m, 7H), 2.37(s, 3H); ^{13}C NMR-($CDCl_3$) δ 196.5, 138.3, 135.6, 135.0, 133.6, 131.0, 129.9, 129.2, 128.8, 128.3, 126.5, 64.4, 53.3, 20.3; IR(CCl_4) 3064, 3025, 2916, 1678 cm^{-1}; EI MS 240(M^+, 4.9), 135(90.1), 105(100), 77(66.3).

Preparation of III. The synthetic procedures were the same as that of **II** except that α-phenylacetophenone was used instead of α-(*o*-tolyl)acetophenone. ^{1}H NMR($CDCl_3$) δ 8.03(distorted d, 2H, J = 7.5 Hz), 7.59−7.25(m, 8H), 3.40(d, 1H, J = 5.4 Hz); 3.09(d, 1H, J = 5.4 Hz). ^{13}C NMR($CDCl_3$) δ 194.8, 135.7, 134.4, 133.9, 130.1, 128.9, 128.7, 128.6, 125.5, 63.3, 55.1; IR-(CCl_4) 3064, 2945, 1688 cm^{-1}; EI MS 224(M^+, 5.4), 105(100), 77(68.5).

Photoproducts. Photoproducts generated from the irradiation of **I** and **II** were isolated with either column- or preparative thin-layer chromatography. The white beam from a medium-pressure mercury arc lamp (Hanovia, 450 W) was filtered with an aqueous solution of 2 mM K_2CrO_4 and 1% K_2CO_3 contained in a Pyrex cell of 1-cm path length to select the sample irradiation light of 313 nm. Quantum efficiencies were measured using 0.1 M valerophenone in benzene as an actinometer.[29] Spiro[cyclopropane-1,1′-(2′-phenyl-2′-hydroxy)indane] ($\mathbf{I_p}$): ^{1}H NMR($CDCl_3$) δ 7.65−6.75(m, 9H), 3.83, 3.43(AB quartet, 2H, J = 16.8 Hz), 2.41(s, 1H, −OH), 1.20−0.59(m, 4H); ^{13}C NMR-($CDCl_3$) δ 146.5, 144.1, 140.6, 128.4, 127.8, 127.4, 126.9, 126.6, 125.2, 119.6, 84.2, 50.2, 39.8, 18.9, 11.0; IR(KBr) 3553, 1485 cm^{-1}; EI MS 236(M^+, 29.3), 218(14.7), 208(42.0), 105(100), 77(33.3). *Z*-3-hydroxy-1-phenyl-2-*o*-tolylpropenone ($\mathbf{II_{p2}}$): ^{1}H NMR($CDCl_3$) δ 16.2(d, 1H, J = 5.0 Hz), 8.59(d, 1H, J = 5.0 Hz), 7.39−7.16(m, 9H), 2.03(s, 3H); ^{13}C NMR($CDCl_3$) δ 185.7, 183.6, 137.9, 135.7, 134.9, 131.7, 131.5, 130.6, 128.7, 128.3, 128.1, 126.6, 114.7, 20.2; IR(KBr) 3460, 3063, 2927, 1727, 1681 cm^{-1}; EI MS 238(M^+, 0.7), 210(9.9), 105(100), 77(34.6).

Materials. Cyclohexane, ethanol, 2,5-dimethyl-2,4-hexadiene (DH), and methyl viologen dichloride ($MVCl_2$), purchased from the Sigma, were used as received. Sample concentration was 5 × 10^{-3} M if not specified otherwise, and solvent was cyclohexane in kinetic measurements except that ethanol was used as solvent with the presence of $MVCl_2$. Samples were contained in 10-mm cells for static measurements, while they were in 2-mm cells for time-resolved measurements.

Static Measurements. Absorption-spectra changes with irradiation were monitored by measuring absorption spectra at scheduled intervals with a UV/vis spectrophotometer (Scinco, S-2040) while directing 2.5-mW white beam from 300-W Xe lamp (Schoeffel, LPS 255) to a sample with the spot diameter of 5 mm. Fluorescence spectra were obtained using a home-built fluorometer, which consists of a 75-W Xe lamp (Acton Research, XS 432), 0.15-m and 0.30-m monochromators (Acton Research, SpectroPro-150 and 300), and a photomultiplier tube (Acton Research, PD 438).

Picosecond Kinetic Measurements. An actively/passively mode-locked Nd:YAG laser (Quantel, YG 701) with the pulse duration of 25 ps was employed for picosecond fluorescence and transient-absorption kinetic measurements. Samples were excited with 266-nm laser pulses or 320-nm pulses generated from a Raman shifter filled with 20-atm methane gas. Fluorescence was collected from the front surface of the sample excitation for all static and time-resolved fluorescence measurements. Fluorescence kinetic profiles were obtained with a 10-ps streak camera (Hamamatsu, C2830) attached with a CCD (Princeton Instruments, RTE-128-H). Transient absorption of a sample was probed using fluorescence from an organic dye excited with the pulses split from sample-excitation pulses. The comparison of dye-emission kinetic profiles measured with streak camera without and with sample excitation yields picosecond transient-absorption kinetic profiles.[30] Fluorescence and transient-absorption kinetic constants were extracted by fitting measured kinetic profiles to computer-simulated kinetic curves convoluted with the temporal response functions.

Nanosecond Spectral Measurements. Transient-absorption spectra were obtained by monitoring the transmittance changes of samples excited made with 266-nm pulses from a 6-ns Q-switched Nd:YAG laser (Quanta System, HYL-101). Probe pulses emitted from an organic dye excited with the pulses split from sample-excitation pulses were detected with a CCD (Princeton Instruments, ICCD-576-G) attached to a 0.5-m spectrometer (Acton Research, SpectroPro-500).

Theoretical Calculation. Deprotonation enthalpies of some selected groups in the molecules **I** and **II**, as well as the ring-opening enthalpies of their intermediates, were calculated semiempirically using the Parameterized Model 3 of MOPAC 97 (Fujitsu).

Results

Photoproduct of I. The ketone **I** is shown to yield only one isolated product, $\mathbf{I_p}$ with IR, NMR, and mass spectroscopy. Observation of the clean conversion is somewhat surprising, since α-(*o*-tolyl)isobutyrophenone, which structurally resembles **I**, is known to give only α-cleavage products.[31] We postulate that the conjugation between carbonyl and cyclopropyl strength-

ens the connecting bond and retards the α-cleavage process.[1] Formation of $\mathbf{I_p}$ from **I**, with the quantum yield (Φ) of 0.14, can be explained with hydrogen abstraction of the excited carbonyl group from the *o*-tolyl group followed by coupling of two radical sites of the biradical intermediate (eq 1), as proposed in the photochemistry of α-(*o*-tolyl)acetophenone.[32]

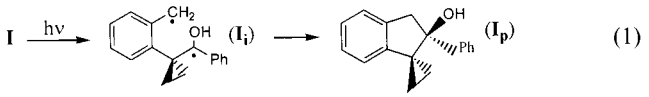

(1)

Photoproducts of II. Judging from TLC analysis, preparative scale irradiation of **II** under the same condition results in a complex mixture of photoproducts. However, after column chromatography using silica gel, only one product has been isolated purely enough to identify the structure. Quantitative analysis has shown that more than 70% of whole products are this product. Spectroscopic data have led us to assign it as $\mathbf{II_{p2}}$. To examine the reaction more closely, we took the ^{1}H NMR of 0.02 M **II** in benzene-d_6, contained in an NMR tube under irradiation, at scheduled intervals. In addition to $\mathbf{II_{p2}}$, formation of another major product was apparent from the ^{1}H NMR spectra (eq 2). It has been assigned to a spiro epoxyindanol ($\mathbf{II_{p1}}$) from the fact that it shows an AB quartet at 3.3−3.5 ppm and two doublets at 2.66 and 2.57 ppm. While only one set of AB quartet was observed in the ^{1}H NMR spectrum of the reaction mixture, the stereochemistry of the product could not be determined due to its instability. The AB quartet is typical of 2-phenyl-2-indanols, as seen in many photolysis examples of α-(*o*-alkylphenyl)acetophenones.[31,32] The assignment is reasonable not only because the NMR spectrum fits into the structure but also because **I**, that is almost identical to **II** geometrically, shows analogous reactivity. The yield ratio of $\mathbf{II_{p1}}$/$\mathbf{II_{p2}}$ was 3/2, and the quantum yield of $\mathbf{II_{p2}}$ was 0.05. If the sample with a small amount of the starting ketone remaining was kept in dark for several days, the peaks corresponding to $\mathbf{II_{p1}}$ diminished considerably, and the growth of peaks for $\mathbf{II_{p2}}$ was noticeable in reference to the peaks of starting ketones. If a crystal of *p*-toluenesulfonic acid was added to the sample, disappearance of $\mathbf{II_{p1}}$ was accelerated considerably. It may be the reason $\mathbf{II_{p1}}$ escaped our efforts to isolate using column chromatography in preparative scale photolysis. The rearrangement from $\mathbf{II_{p1}}$ to $\mathbf{II_{p2}}$ is not common in organic chemistry, and we have no definite clue to the mechanism of the transformation at this moment.

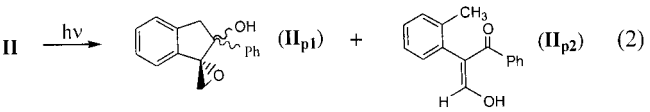

(2)

There could be several reaction pathways possible for the formation of $\mathbf{II_{p2}}$ from **II**. Singlet excited states are reported to be responsible for analogous rearrangements of alkyl ketones with substituted oxirane conjugation.[33] However, intersystem crossing from excited singlet states to triplet states is extremely efficient for phenyl ketones; therefore, the reaction pathway from the first excited singlet state would be negligible. At any rate, no experimental evidences have been observed on the singlet-state reaction (vide infra). More likely mechanisms would be

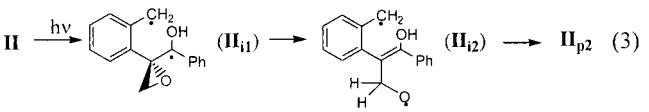

(3)

hydrogen abstraction, ring-opening, and disproportionation such as eq 3.

Photoproducts of II(d_2). To see if this mechanism is really working, **II(d_2)** was prepared and irradiated under the same conditions. The ^{1}H NMR spectrum of the major photoproduct isolated with column chromatography was essentially the same as that of $\mathbf{II_{p2}}$ except that the peak at 16.02 ppm became singlet and that the peak at 8.59 ppm was absent. A careful examination of the spectrum has revealed that a singlet at 2.02 ppm overlaps with a broad triplet with an equal intensity. The ^{13}C NMR spectrum of the sample also showed a similar pattern at 20 ppm. The triplet patterns of both ^{1}H- and ^{13}C NMR spectra clearly suggest that a ^{2}H atom is incorporated at the benzylic methyl group of $\mathbf{II_{p2}}$, and the overlap of the singlet and the triplet tells us that the sample contains two types of $\mathbf{II_{p2}(d_2)}$ as shown below. The yield ratio of $\mathbf{II_{p2}(d_2A)/II_{p2}(d_2B)}$, which was obtained integrating the ^{1}H NMR peaks at 2.02 and 16.02 ppm, was 1.

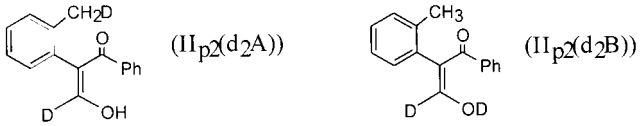

Formation of $\mathbf{II_{p2}(d_2A)}$ from **II(d_2)** could be explained by the mechanism of eq 3. However, the reaction pathway to $\mathbf{II_{p2}(d_2B)}$ was not obvious at this stage. One possible route to $\mathbf{II_{p2}(d_2B)}$ would be hydrogen abstraction from the oxiranyl ring followed by ring-opening (eq 4). Even though this type of reaction sequence has been ignored in the photochemistry of α,β-oxiranyl ketones, it is still probable especially in the case of phenyl ketones with acidic hydrogen atoms nearby. Our theoretical results also support this idea (vide infra). To obtain experimental evidences for this mechanism, **III** was prepared and irradiated under the same reaction condition. As expected, a β-hydroxy enone ($\mathbf{III_p}$) was isolated as a major product. Involvement of singlet-excited states also could be ruled out by the fact that the reaction was quenched by triplet quenchers such as DH.

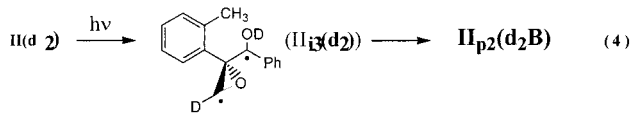

(4)

Picosecond Kinetics. The cyclohexane solutions of **I** and **II** show fluorescence decaying in 70 and 25 ps, respectively (Figure 1). Because of these short lifetimes the fluorescence quantum efficiencies are too low to observe the static fluorescence of the reactants buried under long-lived luminescence from impurities such as photoproducts. The photolyzed cyclohexane solutions of **I** and **II** expose product fluorescence spectra with the peaks at 390 and 370 nm, respectively. The short fluorescence lifetimes of both reactants suggest that, following unresolvably fast internal conversion from the S_2 states, the population of the $S_1(n,\pi^*)$ states undergoes a rapid intersystem crossing to the $T_2(\pi,\pi^*)$ states that happen to lie near the S_1 states in energy. The El-Sayed rule,[34] that the intersystem crossing transition of $S_1(n,\pi^*)$-to-$T(\pi,\pi^*)$ is allowed, also supports that the fast lifetimes of the S_1 states are resulting from rapid intersystem crossing. The shorter fluorescence lifetime (25 ps) of **II**, compared with that (70 ps) of **I**, implies that **II** undergoes intersystem crossing more rapidly, probably owing to its more nonbonding character at the S_1 state introduced with the additional oxygen atom in the small ring.

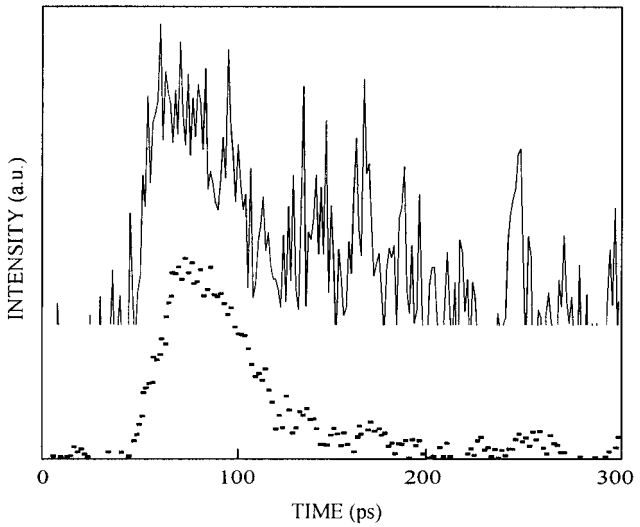

Figure 1. Fluorescence kinetic profiles at 450 nm of **I** (solid) and **II** (dotted) in cyclohexane. **I** and **II** were excited at 320 and 266 nm, respectively. The convoluted decay time constants of **I** and **II** are 70 and 25 ps, respectively.

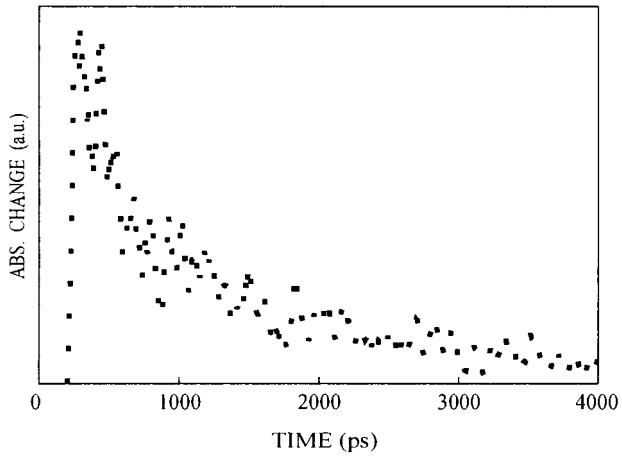

Figure 2. Transient-absorption kinetic profile, excited at 266 nm and collected at 400 nm, of **I** in cyclohexane. A biexponential decay of 0.6 ns (92%) and 20 ns (8%) fits to the profile.

The faster decay component (0.6 ns) of transient absorption at 400 nm, shown in Figure 2, is assigned to the T_1-state decay of **I**, while the slower one with small amplitude is assigned to the decay of the succeeding intermediate $\mathbf{I_i}$ as shown in Figure 3. The decay kinetics of the T_1 state could not be measured for **II**. The transient absorption of quencher-free **I** at 350 nm decays with the time constant of 20 ns, and this is attributed to the transient $\mathbf{I_i}$ (Figure 3). To understand the nature of the intermediate $\mathbf{I_i}$, we have also measured the effects of quenchers on the transient-absorption kinetic profile. The drastic quenching of the transient-absorption signal with 1.0 M DH suggests that the precursor of $\mathbf{I_i}$ is the lowest triplet state of **I**. The reaction at the T_1 state is intramolecular hydrogen transfer from the methyl group to the carbonyl group. The time of 0.6 ns is quite short for hydrogen abstraction to occur at a triplet state. The fast abstraction becomes possible with the increased acidity of the methyl group in the tolyl group and the increased basicity of the carbonyl group at the first excited triplet state.[35−38] The decay time of 2.5 ns observed in the presence of $MVCl_2$, a type of saturated radical quencher, is much shorter than that without $MVCl_2$. However, the presence of $MVCl_2$ does not reduce the absorption signal at zero delay time at all. The significant reduction in the decay time and the same signal in the initial absorbance imply that the intermediate $\mathbf{I_i}$ is a radical, more specifically a biradical in nature. We will show the effect of $MVCl_2$ on the spectrum of $\mathbf{I_i}$ in the later part of this paper. The decay time of 20 ns is ascribed to the cyclization time of intermediate $\mathbf{I_i}$ to transform into the photoproduct $\mathbf{I_p}$.

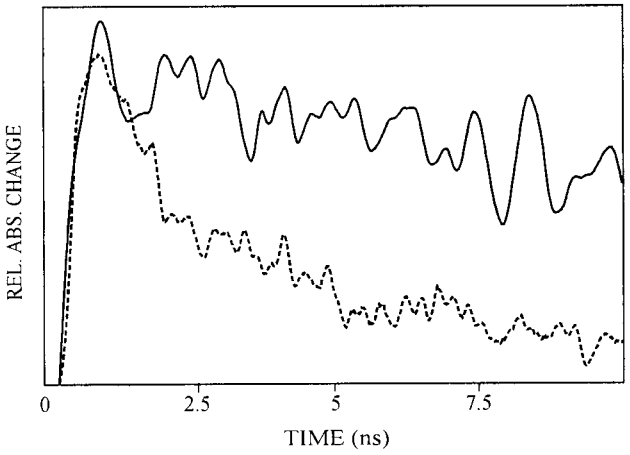

Figure 3. Transient-absorption kinetic profiles, excited at 266 nm and monitored at 350 nm, of **I** in cyclohexane without (solid) and with $MVCl_2$ (dotted). The solid profile has a decay time of 20 ns, while the dotted profile decays in 2.5 ns.

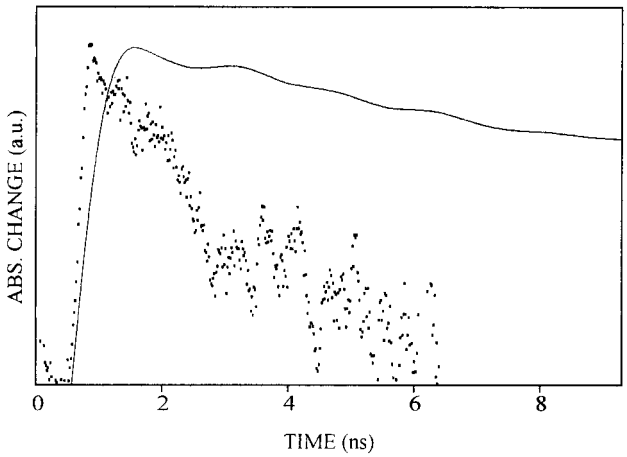

Figure 4. Transient-absorption kinetic profiles of **II** in cyclohexane with 266-nm excitation. The kinetics at 320 (solid) and 350 nm (dotted) have decay times of 27 and 2.3 ns, respectively.

Figure 4 shows that the transient absorption at 350 nm of **II** decays much faster (with the time of 2.3 ns) than that of **I** given in Figure 3. Furthermore, the transient absorption at 320 nm with the decay time of 27 ns suggests that there is an additional photolyzed transient ($\mathbf{II_{i2}}$) besides the $\mathbf{II_{i1}}$. The decay time of 2.3 ns at 350 nm is assigned to the transformation time of $\mathbf{II_{i1}}$ into $\mathbf{II_{i2}}$ and $\mathbf{II_{p1}}$, while the decay time of 27 ns at 320 nm is ascribed to the transformation time of $\mathbf{II_{i2}}$ into $\mathbf{II_{p2}}$. The transient absorption at 320 nm rises more slowly than that at 350 nm. The slow formation of $\mathbf{II_{i2}}$ transient absorption is contributing to the relatively slow rising kinetics at 320 nm. The quenching effects of DH and $MVCl_2$ on the transient absorption of **II** are similar to those on the transient absorption of **I**.

Nanosecond Transient Absorption Spectra. For better understanding of photochemical reaction intermediates, we have also measured time-resolved transient-absorption spectra besides kinetic profiles. The transient-absorption spectra in Figure 5 expose that the intermediate $\mathbf{I_i}$ contains the 350-nm absorption band of hydroxybenzyl radical chromophore as well as the 320-nm band of benzyl radical chromophore.[39−41] This again supports that the intermediate $\mathbf{I_i}$ is a biradical.

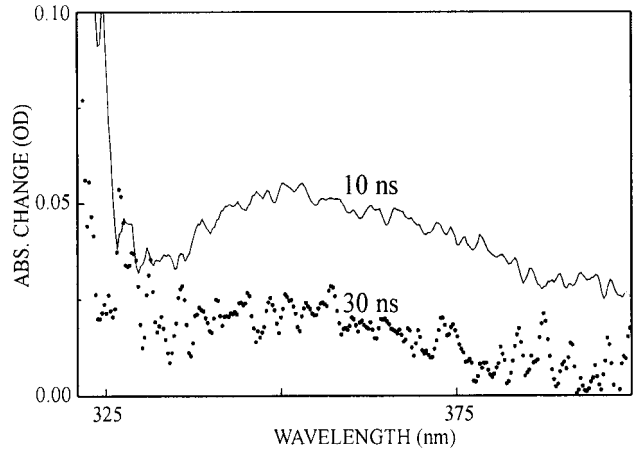

Figure 5. Transient-absorption spectra of **I** in cyclohexane at the shown delay times after 266-nm excitation.

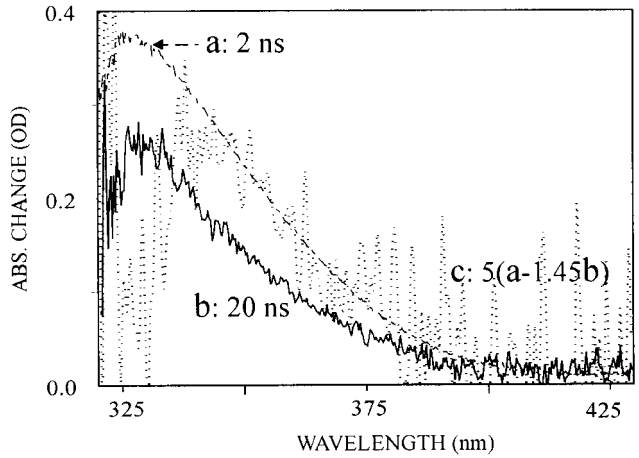

Figure 6. Transient-absorption spectra of **II** in cyclohexane at 2- **(a)** and 20-ns **(b)** delay times after 266-nm excitation and a difference spectrum **(c)** simulated from 5 (a − 1.45b).

However, the transient-absorption spectra of **a** and **b** in Figure 6 are much stronger and shifted to the blue with the peak at 330 nm, compared with the 350-nm absorption band in Figure 5. We ascribe the transient absorption in the spectra **a** and **b** mainly to the biradical of $\mathbf{II_{i2}}$. The 330-nm absorption band of $\mathbf{II_{i2}}$ is mainly attributable to the olefin conjugated with phenyl and benzyl radical chromophores because the maximum-absorption wavelength and the large extinction coefficient resemble those of stilbenes. The absorption band of the benzyl chromophore of $\mathbf{II_{i1}}$ is buried under the strong absorption band with the peak at 330 nm, as the transient absorption resulting from $\mathbf{II_{i1}}$ decays too fast to measure directly with our spectrometer of 6-ns temporal resolution. However, we can simulate its spectrum as **c** in Figure 6, on the basis of the assumption that the transient-absorption spectrum at 2 ns contains more contribution of the fast decaying $\mathbf{II_{i1}}$ than that at 20 ns. Nevertheless, the spectrum **c** displays the buried absorption band of hydroxybenzyl radical chromophore. This implies that **II** at T_1 state can undergo intramolecular hydrogen transfer to yield the biradical $\mathbf{II_{i1}}$. $\mathbf{II_{i1}}$ then undergoes ring-opening to form the biradical of $\mathbf{II_{i2}}$ as well as cyclization to produce the product $\mathbf{II_{p1}}$.

Transient-absorption bands arising from $\mathbf{I_i}$ and $\mathbf{II_{i2}}$ are quenched by $MVCl_2$ (Figure 7) to give birth to a new absorption band of reduced methyl viologen cation with the peak at 620 nm (Figure 8). The transient-absorption decay times of $\mathbf{I_i}$ and $\mathbf{II_{i2}}$ are not reduced by the presence of DH. However, the

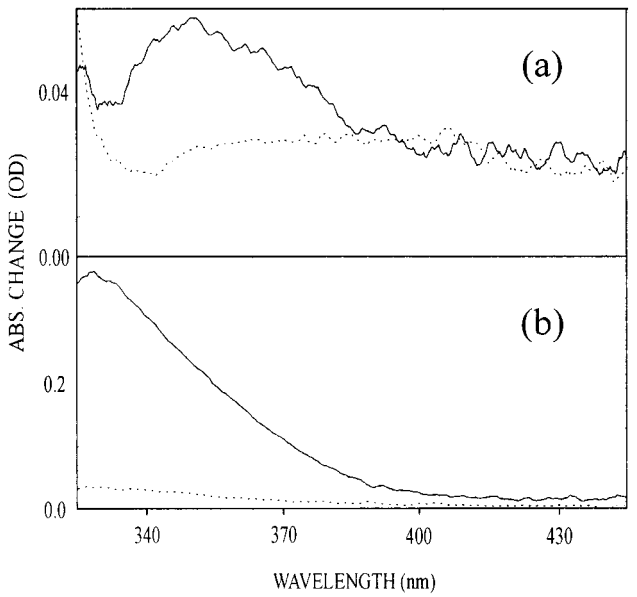

Figure 7. Transient-absorption spectra, at 10-ns delay after 266-nm excitation, of **I** (a) and **II** (b) in cyclohexane (solid) and in the 19:1 (v:v) mixture of cyclohexane and $MVCl_2$-saturated ethanol (dotted).

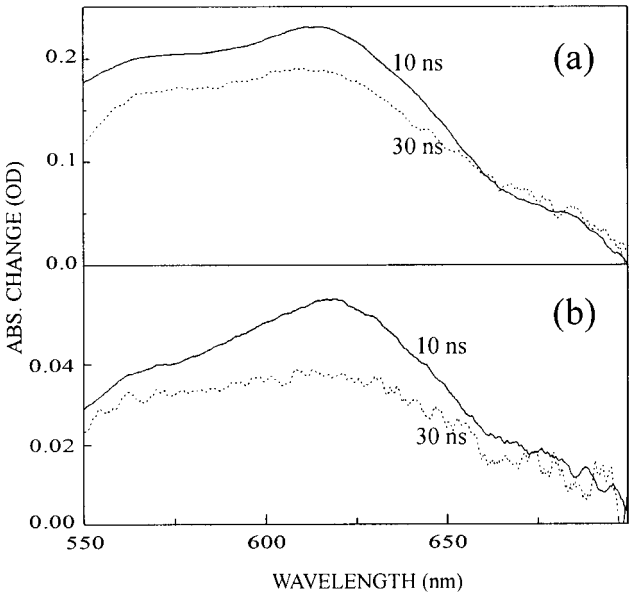

Figure 8. Transient-absorption spectra of $MVCl_2$ (1×10^{-3} M) ethanol solutions with **I** (a) and **II** (b) at two given delay times after 266-nm excitation.

amplitudes of the signals are reduced with the concentration increase of DH as discussed already. These facts also support that all of the reaction intermediates of $\mathbf{I_i}$, $\mathbf{II_{i1}}$, and $\mathbf{II_{i2}}$ have a T_1 state as a precursor at a time and that they are biradicals indeed.

Static Absorption Changes with Irradiation. The absorption spectrum of **II** in cyclohexane changes significantly with irradiation, while that of **I** in cyclohexane does not (Figure 9). A significant increase in the extinction coefficient of the lowest absorption band with irradiation suggests that the transition of $S_1 \leftarrow S_0$ in a product has more conjugation with more (π,π^*) character than that in the reactant **II**. A negligible change with irradiation in the absorption spectrum of sample **I** agrees with the fact that the absorption chromophores of the product $\mathbf{I_p}$ in the low energy region are very similar to those of the reactant **I**. The observations in Figure 9 agree with the photoproduct

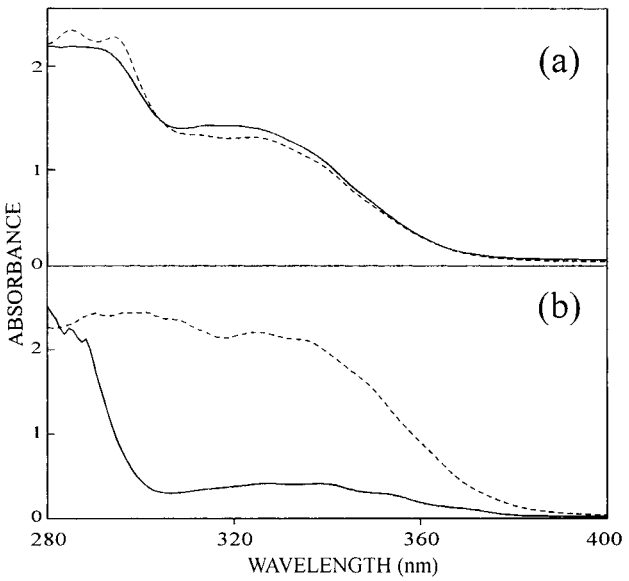

Figure 9. Absorption spectra of cyclohexane solutions of **I** (a) and **II** (b) without (solid) and with irradiation (dashed).

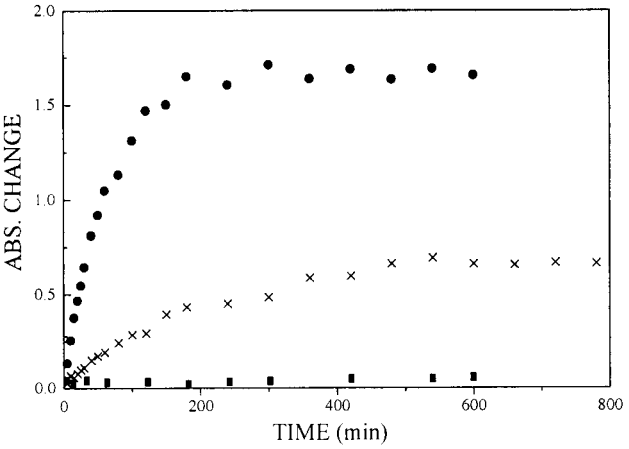

Figure 10. Absorption changes with time at 320 nm for the 2.5×10^{-3} M cyclohexane solutions of **II** (●), **III** (×), and **III** with 1.0 M DH (■) under the same irradiation conditions. The profile of **II** converges to 1.7 with a time constant of 75 min, while that of **III** (×) to 0.7 with a time constant of 200 min.

analyses[16] that **II** forms more conjugated photoproduct $\mathbf{II_{p2}}$, while **I** produces the cyclized photoproduct $\mathbf{I_p}$.

As shown in product studies, $\mathbf{II(d_2)}$ produces three different photoproduct isomers. As the methylene group of the oxiranyl ring was speculated to be acidic for the carbonyl group to abstract a hydrogen atom from the oxiranyl ring, the absorption changes of the **II** and **III** samples with irradiation time were compared at 320 nm. Although the amplitude and rate of the absorption rise are smaller for **III** than for **II**, Figure 10 clarifies that **III** produces the photoproduct corresponding to $\mathbf{II_{p2}}$ without having the methyl group. This confirms the earlier suggestion that intramolecular hydrogen transfer from the oxiranyl ring to the carbonyl group can also occur to produce an intermediate ($\mathbf{II_{i3}}$) at the T_1 state of **II**, together with the transfer from the methyl group to the carbonyl group. $\mathbf{II_{i3}(d_2)}$ is suggested to rearrange into the product $\mathbf{II_{p2}(d_2B)}$ immediately.

Discussion

Rate Constants. Observed time constants were used with quantum efficiencies and product yield ratios to calculate the rate constants of individual elementary reactions. As the transition between $S_1(n,\pi^*)$ and $T_2(\pi,\pi^*)$ is allowed by the El-Sayed rule,[34] the quantum efficiency of the T_1 state population is assumed to be about 1. Then the quantum efficiency (0.14) of the only product $\mathbf{I_p}$ should be the fraction of $\mathbf{I_i}$ formation rate constant to the observed decay rate constant, $(0.6\ \text{ns})^{-1}$, of T_1 state. The resulting rate constants of hydrogen abstraction and intersystem crossing to the S_0 state are 2.3×10^8 and $1.4 \times 10^9\ s^{-1}$, respectively. The intersystem crossing is very fast as expected again with the El-Sayed rule[30] that the transition between $T_1(n,\pi^*)$ and $S_0(n^2)$ is allowed. The other rate constants can be automatically calculated as the inverse of the observed time constants.

TABLE 1: Calculated Deprotonation Enthalpies of Some Selected Groups in I and II

molecule	group	distance[a]	$\Delta H^b(S_0)$	$\Delta H(T_1)$	$\Delta H(T_1) - \Delta H(S_0)$
I	$C_{(1)}H_3$	2.9	351	348	−3
	$C_{(2)}H_2$	2.7	359	358	−1
	$C_{(3)}H$	2.8	375	358	−17
	$O_{(1)}H^+$		186	212	26
II	$C_{(1)}H_3$	2.7	347	313	−34
	$C_{(2)}H_2$	3.0	355	329	−26
	$C_{(3)}H$	2.5	374	360	−14
	$O_{(1)}H^+$		184	243	59

[a] From the closest hydrogen atom of each group to $O_{(1)}$ in Å. [b] Deprotonation enthalpy in kcal/mol.

It has been shown that the quantum yield of $\mathbf{II_{p2}}$ is 0.05, while the product yield ratios of $\mathbf{II_{p1}/II_{p2}}$ and $\mathbf{II_{p2}(d_2B)/II_{p2}(d_2A)}$ are 1.5 and 1, respectively. Since we could measure neither the decay time of the T_1 state nor any formation times of $\mathbf{II_{i1}}$ and $\mathbf{II_{i3}}$, we cannot calculate hydrogen-transfer rate constants without assuming that the formation rate constants of $\mathbf{I_i}$ and $\mathbf{II_{i1}}$ are the same. The assumption is reasonable as the substitution of an oxygen atom in the three-membered ring, which is distant from the methyl group, would not affect the acidity of the methyl group significantly. With the assumption, the formation rate constant of $\mathbf{II_{i3}}$ is estimated to be $6.7 \times 10^7\ s^{-1}$, as the quantum yield of $\mathbf{II_{p2}(d_2B)}$ produced from $\mathbf{II_{i3}}$ is one-fourth of the total quantum yield of $\mathbf{II_{p1}}$ and $\mathbf{II_{p2}(d_2A)}$ produced from $\mathbf{II_{i1}}$. The relative quantum yields of $\mathbf{II_{p1}}$ and $\mathbf{II_{p2}(d_2A)}$ with the decay time of $\mathbf{II_{i1}}$ allow us to calculate the rate constants of the ring-opening and cyclization processes of $\mathbf{II_{i1}}$ as well. The other rate constants can be trivially calculated.

Theoretical Consideration. Thus far we have experimentally shown that the photolysis reactions of **II** are dramatically different from those of **I**. The only structural change in **II** is the substitution of an oxygen atom for the methylene group of the three-membered ring in **I**. A simple semiempirical calculation reveals that the drastic changes in the reactions are a result of the significantly increased acidity and instability of the small ring with the oxygen substitution. Table 1 shows that a proton of $C_{(2)}H_2$ becomes very acidic at the T_1 state of **II**, while that at the T_1 state of **I** is not. Because of this acidity increment, the new reaction pathway of $\mathbf{II_{p2}(d_2B)}$ product formation can occur within the short T_1 lifetime of **II**. It should be mentioned that deprotonation enthalpies instead of dehydrogenation enthalpies were calculated to avoid spin contamination in our low-level calculation. We can also note from Table 1 that both the acidity of the methyl group and the basicity of the carbonyl group increase very significantly in the excited triplet state, explaining that all of the hydrogen-transfer reactions at the T_1 states of **I** and **II** are plausible. Table 2 reveals the reason that **II** undergoes the ring-opening while **I** does not. The ring rupture is energetically very favorable for $\mathbf{II_{i1}}$, but it is not at all for $\mathbf{I_i}$. We have also noticed that a C−H bond length of the oxiranyl ring of $\mathbf{II_{i1}}$ is to extend as long as 1.9 Å after the ring-opening,

TABLE 2: Calculated Enthalpy Changes with Three-Membered Ring Ruptures

molecule	closed intermediate	opened intermediate	ΔH^a
I	I_i	$\mathbf{I}_i$[b]	3
II	II_{i1}	$\mathbf{II}_{i2}$[c]	−30

[a] Enthalpy change in kcal/mol. [b] The biradical intermediate of **I** corresponding to $\mathbf{II}_{i2}$ of **II**. [c] A $C_{(2)}$−H bond of $\mathbf{II}_{i1}$ is to extend as long as 1.9 Å after the ring-opening, indicating that the bond is very acidic.

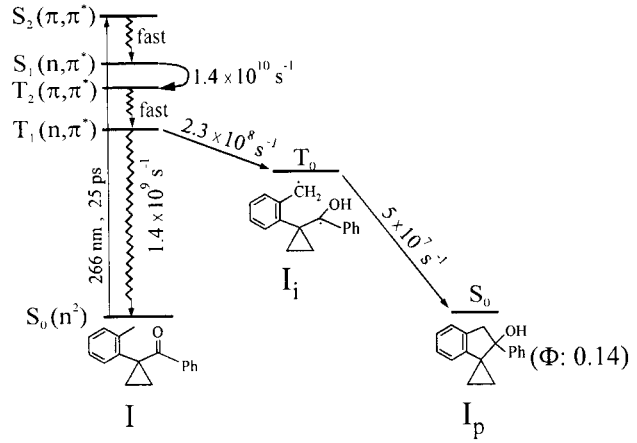

Figure 11. Schematic photolysis mechanism of 1-(*o*-tolyl)-1-benzoylcyclopropane in cyclohexane.

indicating that the bond becomes very acidic. Although the $C_{(2)}$−H bond is acidic from the reactant form of **II**, its acidity increases further with the ring rupture. The acidity increase expedites the hydrogen-transfer reaction of $\mathbf{II}_{i2}$ obviously.

Photolysis Mechanism. Photoexcitation of **I** and **II** in cyclohexane leads to the photolysis reactions through the pathways with the rate constants of the individual elementary reactions shown in Figures 11 and 12, respectively. Following rapid internal conversion from the UV-excited $S_2(\pi,\pi^*)$ states, the $S_1(n,\pi^*)$ states of **I** and **II** molecules undergo intersystem crossing in 70 and 25 ps, respectively, to populate the T_1 states. **I** at T_1 goes through intramolecular hydrogen transfer from the methyl group to the carbonyl group to produce a biradical intermediate with a rate constant of 2.3×10^8 s^{-1}. The intermediate transforms into a cyclized photoproduct $\mathbf{I}_p$ at 5×10^7 s^{-1}. The low quantum efficiency of $\mathbf{I}_p$ formation (0.14) is a result of the small hydrogen-abstraction rate compared with the intersystem crossing rate of the T_1 state. On the other hand, the carbonyl group of **II** at T_1 can abstract a hydrogen atom from the oxiranyl ring to form another biradical intermediate $\mathbf{II}_{i3}$ at a rate constant of 6×10^7 s^{-1}, or from the methyl group to form $\mathbf{II}_{i1}$ at 2.3×10^8 s^{-1}. The additional reaction channel of $\mathbf{II}_{i3}$ formation is opened as a result of the acidity increase of the oxiranyl ring with oxygen substitution. While $\mathbf{II}_{i3}(\mathbf{d}_2)$ produces immediately a rearranged product of $\mathbf{II}_{p2}(\mathbf{d}_2\mathbf{B})$ with a quantum efficiency of 0.025, $\mathbf{II}_{il}$ transforms into a cyclized product of $\mathbf{II}_{p1}$ with a quantum efficiency of 0.075 at a rate constant of 3.3×10^8 s^{-1}. (The product $\mathbf{II}_{p1}$ undergoes rearrangement to form $\mathbf{II}_{p2}$ in a very slow time scale.) However, the opening process of the oxiranyl ring also competes with the cyclization process at a rate constant of 1.1×10^8 s^{-1} to form a new biradical intermediate of $\mathbf{II}_{i2}$. The ring-opening becomes fast enough to compete with the cyclization, as the three-membered ring of the biradical intermediate becomes extremely unstable with oxygen presence. $\mathbf{II}_{i2}(\mathbf{d}_2)$ then undergoes intramolecular hydrogen transfer at a rate constant of 3.7×10^7 s^{-1} to form another product of $\mathbf{II}_{p2}(\mathbf{d}_2\mathbf{A})$ with a quantum yield of 0.025. The acidity increase of a $C_{(2)}$−H bond in the oxiranyl ring with the ring-opening expedites the formation rate of $\mathbf{II}_{p2}$ from $\mathbf{II}_{i2}$. The photolysis reactions of **II** are extremely different from those of **I**. They are much more complicated and faster overall than reactions of **I**. All of these changes are driven by the drastic ring-activation effect of oxygen substitution in the three-membered ring.

Physical Meanings. Bowry et al. have shown that the ring-opening process of α-phenyl cyclopropylcarbinyl radicals set an equilibrium favoring the cyclic forms.[42] More recently, the cyclization rate constant at 20 °C is reported to be 5.4×10^6 s^{-1}.[25] These results fit nicely into our observation that in the photochemical reaction of **I** the biradical intermediate $\mathbf{I}_i$ cyclizes to $\mathbf{I}_p$ at a rate of 5×10^7 s^{-1} without opening the cyclopropyl ring. The oxiranylcarbinyl radical ring-opening were known to be much faster than the cyclopropylcarbinyl radical rearrangement.[21−23] Our kinetic study of **II** also shows that $\mathbf{II}_{i1}$, a biradical intermediate from **II**, opens up the oxiranyl ring at a rate of 1.1×10^8 s^{-1}, which is now able to compete with the biradical closure. This number is smaller by 2 orders of magnitude than 3.2×10^{10} s^{-1} of an alkyl-substituted oxiranylcarbinyl radical reported by Rawal.[22] Both phenyl and hydroxy substituents of

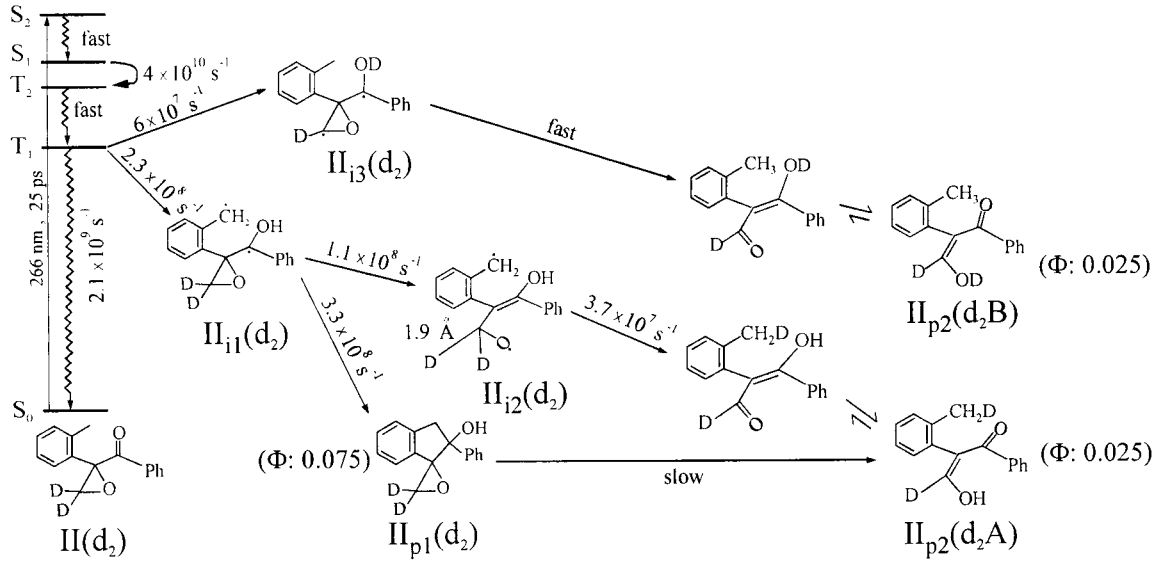

Figure 12. Schematic photolysis reaction mechanism of $^2H_2$-substituted 2-(*o*-tolyl)-2-benzoyloxirane in cyclohexane.

$\mathbf{II_{i1}}$ are considered to be responsible for the reduced rate.[43−46] The reaction dichotomy between **I** and **II** is interesting in contrast to the photochemistry of 1-benzoyl-2,2-dimethylcyclopropane[1] and 2-benzoyl-3,3-dimethyloxirane.[19] The latter ketones are known to give similar photochemical rearrangements (eqs 5 and 6), where both cyclopropyl and oxiranyl rings open up following hydrogen abstraction from the γ-position. In these cases, the ring closure of the biradical intermediates could not compete with the ring-opening due to energetically unfavorable bicyclic products.

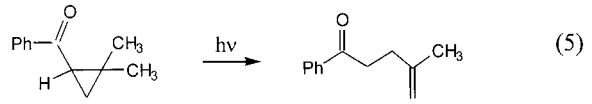

(5)

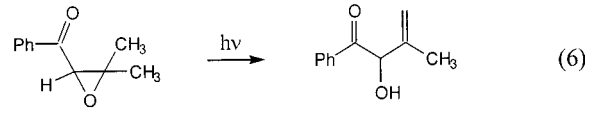

(6)

There are three different routes leading to $\mathbf{II_{p2}}$ from **II**, where $\mathbf{II_{p2}(d_2A)}$ becomes identical to $\mathbf{II_{p2}(d_2B)}$ with nondeuterated **II** (Figure 12). All of the three routes are unique features of **II**, which have not been discussed until now in the photoinduced rearrangement of the conjugated oxiranyl ketones to 1,3-dicarbonyl compounds. This type of rearrangement was explained in the frame of singlet excited states so far.[33] Our current study shows that the same skeletal rearrangement can occur via a hydrogen-abstraction reaction from excited triplet states, which have been ignored mostly in the previous works. The oxiranyl ring-openings induced by hydrogen-abstraction reactions have been described for a few α,β-oxiranyl ketones[19] and β,γ-oxiranyl ketones,[47] but they all are known to undergo different types of rearrangements. The main difference is that, whereas all of the previous examples involve 1,4-biradical intermediates, our current one involves either the 1,3- or the 1,5-biradical intermediate.

Regarding the differences in the behaviors of $\mathbf{I_i}$ and $\mathbf{II_{i1}}$, it is also interesting to note that the cyclization rate of $\mathbf{II_{i1}}$ is faster than that of $\mathbf{I_i}$ by a factor of 7 despite the similarity of two structures. Caldwell et al. have shown from their study on the photochemistry of valerophenone and α-ethoxyacetophenone that the intervening oxygen can decrease the lifetime of biradical intermediates.[48] It would be interesting to find out how important the epoxy−oxygen bridge in $\mathbf{II_{i1}}$ is in the determination of the 1,5-biradical lifetime. Obviously, more studies have to be done to evaluate the oxygen effect in this regard. We are currently investigating into this matter with other substrates.

Conclusions

Structurally analogous **I** and **II** show a mechanistic dichotomy in their photolysis reactions. **I** yields a single photoproduct, while $\mathbf{II(d_2)}$ gives birth to three different photoproducts. Following rapid internal conversion from S_2 states, the $S_1(n,\pi^*)$ states of **I** and **II** undergo intersystem crossing in 70 and 25 ps, respectively. **I** at T_1 undergoes intramolecular hydrogen transfer at 2.3×10^8 s^{-1} from the methyl group to the carbonyl group to form a biradical intermediate, which transforms into a cyclized photoproduct (Φ 0.14; 5×10^7 s^{-1}). However, the carbonyl group of **II** at T_1 can abstract a hydrogen atom from the oxiranyl ring (6×10^7 s^{-1}) as well as from the methyl group (2.3×10^8 s^{-1}). The biradical intermediate $\mathbf{II_{i3}}$ from the former process immediately rearranges into a photoproduct $\mathbf{II_{p2}(B)}$ (Φ 0.025), while the intermediate $\mathbf{II_{i1}}$ from the latter transforms into a new oxiranyl ring-opened intermediate $\mathbf{II_{i2}}$ (1.1×10^8 s^{-1}) or a cyclized photoproduct $\mathbf{II_{p1}}$ (Φ 0.075; 3.3×10^8 s^{-1}). ($\mathbf{II_{p1}}$ rearranges into $\mathbf{II_{p2}}$ at a slow rate.) $\mathbf{II_{i2}}$ transforms into another photoproduct $\mathbf{II_{p2}(A)}$ (Φ 0.025; 3.7×10^7 s^{-1}). The dramatic changes of **II** are the result of the increase in the acidity and instability of the three-membered ring with oxygen substitution.

Acknowledgment. We thank the Center for Molecular Catalysis and the Korea Research Foundation (KRF-2000-015-DP0913) for financial support. B.S.P. acknowledges the support from the Korea Science and Engineering Foundation (96-0501-09-01-3). H.K. thanks the Brain Korea 21 Program for a fellowship. We also acknowledge the Equipment Joint Use Program of the Korea Basic Science Institute.

References and Notes

(1) Padwa, A. In *Organic Photochemistry*; Chapman, O. L., Ed.; Marcel Dekker: New York, 1967; Vol. 1, p 91.
(2) Bertoniere, N. R.; Griffin, G. W. In *Organic Photochemistry*; Chapman, O. L., Ed; Marcel Dekker: New York, 1973; Vol. 3, p 115.
(3) Maruyama, K.; Kubo, Y. In *CRC Handbook of Organic Photochemistry and Photobiology*; Horspool, W. M., Song, P.-S., Eds.; CRC: New York, 1994; Chapter 30, p 375.
(4) Hasegawa, E.; Ishiyama, K.; Kato, T.; Horaguchi, T.; Shimizu, T.; Tanaka, S.; Yamashita, Y. *J. Org. Chem.* **1992**, *57*, 5352.
(5) Pandey, B.; Rao, A. T.; Dalvi, P. V.; Kumar, P. *Tetrahedron* **1994**, *50*, 3843.
(6) Cossy, J.; Furet, N.; BouzBouz, S. *Tetrahedron* **1995**, *51*, 11751.
(7) Nastashi, M.; Streith. J. In *Rearrangements in Ground and Excited States*; de Mayo, P., Ed.; Academic Press: New York, 1980; Vol. 3, p 445.
(8) Hasegawa, E.; Ishiyama, K.; Horaguchi, T.; Shimizu, T. *J. Org. Chem.* **1991**, *56*, 1631.
(9) Dauben, W. G.; Shaffer, G. W.; Deviny, E. J. *J. Am. Chem. Soc.* **1970**, *92*, 6273.
(10) Benkeser, R. A.; Hooz, J.; Liston, T. V.; Trevillyan, A. E. *J. Am. Chem. Soc.* **1963**, *85*, 3984.
(11) Paquette, L. A.; Nitz, T. J.; Ross, R. J.; Springer, J. P. *J. Am. Chem. Soc.* **1984**, *106*, 1446.
(12) Hasegawa, E.; Ishiyama, K.; Fujita, T.; Kato, T.; Abe, T. *J. Org. Chem.* **1997**, *62*, 2396.
(13) Kirschberg, T.; Mattay, J. *J. Org. Chem.* **1996**, *61*, 8885.
(14) Williams, J. R.; Sarkisian, G. M.; Quigley, J.; Hasiuk, A.; VabderVennen, R. *J. Org. Chem.* **1974**, *39*, 1028.
(15) Zimmerman, H. E.; Moore, C. M. *J. Am. Chem. Soc.* **1970**, *92*, 2023.
(16) Zimmerman, H. E.; Hixson, S. S.; McBride, E. F. *J. Am. Chem. Soc.* **1970**, *92*, 2000.
(17) Griffin, G. W.; O'Connell, E. J.; Hammond, H. A. *J. Am. Chem. Soc.* **1963**, *85*, 1001.
(18) Griffin, G. W.; Covell, J.; Peterson, R. C.; Dodson, R. M.; Klose, G. *J. Am. Chem. Soc.* **1965**, *87*, 1410.
(19) Zimmerman, H. E.; Cowley, B. R.; Tseng, C.-Y.; Wilson, J. W. *J. Am. Chem. Soc.* **1964**, *86*, 947.
(20) Newcomb, M. *Tetrahedron* **1993**, *49*, 1151.
(21) Krosely, K. W.; Gleicher, G. J. *J. Phys. Org. Chem.* **1993**, *6*, 228.
(22) Krishnamurthy, V.; Rawal, V. H. *J. Org. Chem.* **1997**, *62*, 1572.
(23) Pasto, D. J. *J. Org. Chem.* **1996**, *61*, 252.
(24) Newcomb, M.; Choi, S.-Y.; Horner, J. H. *J. Org. Chem.* **1999**, *64*, 1225.
(25) Halgren, T. A.; Roberts, J. D.; Horner, J. H.; Martinez, F. N.; Tronche, C.; Newcomb, M. *J. Am. Chem. Soc.* **2000**, *122*, 2988.
(26) Chang, D. J.; Koh, E.; Kim, T. Y.; Park, B. S.; Kim, T. G.; Kim, H.; Jang, D.-J. *Tetrahedron Lett.* **1999**, *40*, 903.
(27) Dark, N. L.; Allen, P. *Organic Syntheses*; Wiley: New York, 1955; Collect. Vol. I, p 77.
(28) Corey, E. J.; Chaykovsky, M. *J. Am. Chem. Soc.* **1965**, *87*, 1353.
(29) Wagner, P. J.; Kelso, P. A.; Kemppainen, A. E.; McGrath, J. M.; Schott, H. N.; Zepp, R. G. *J. Am. Chem. Soc.* **1972**, *94*, 7506.
(30) Jang, D.-J.; Kelley, D. F. *Rev. Sci. Instrum.* **1985**, *56*, 2205.
(31) Wagner, P. J.; Zhou, B.; Hasegawa, T.; Ward, D. L. *J. Am. Chem. Soc.* **1991**, *113*, 9640.
(32) Wagner, P. J.; Meador, M. A.; Zhou, B.; Park, B. S. *J. Am. Chem. Soc.* **1991**, *113*, 9630.
(33) Markos, C. S.; Reusch, W. *J. Am. Chem. Soc.* **1967**, *89*, 3363.
(34) El-Sayed, M. A. *J. Chem. Phys.* **1963**, *38*, 2834.

(35) Nakamura, M.; Miki, M.; Majima, T. *J. Chem. Soc., Perkin Trans. 1* **2000**, 415.
(36) Lewis, F. D.; Johnson, R. W.; Kory, D. R. *J. Am. Chem. Soc.* **1974**, *96*, 6100.
(37) Wagner, P. J.; Kemppainen, A. E. *J. Am. Chem. Soc*. **1972**, *94*, 7495.
(38) Wagner, P. J.; Kemppainen, A. E.; Jellinek, T. *J. Am. Chem. Soc*. **1972**, *94*, 7512.
(39) Hatanaka, K.; Itoh, T.; Asahi, T.; Ichinose, N.; Kawanishi, S.; Sasunga, T.; Fukumura, H.; Masuhara, H. *J. Phys. Chem. A* **1999**, *103*, 11257.
(40) Cozens, F. L.; Ortiz, W.; Schepp, N. P. *J. Am. Chem. Soc*. **1998**, *120*, 13543.
(41) Wagner, P. J.; Kelso, P. A.; Zepp, R. G. *J. Am. Chem. Soc*. **1972**, *94*, 7480.
(42) Bowry, V. W.; Lusztyk, J.; Ingold, K. U. *J. Chem. Soc., Chem. Commun.* **1990**, 923.
(43) Halgren, T. A.; Howden, M. E. H.; Medof, M. E.; Roberts, J. D. *J. Am. Chem. Soc*. **1967**, *89*, 3051.
(44) Venkatesan, H.; Greenberg, M. M. *J. Org. Chem*. **1995**, *60*, 1053.
(45) Tanner, D. D.; Chen, J. J.; Lueho, C.; Peters, P. M. *J. Am. Chem. Soc*. **1992**, *114*, 713.
(46) Tanko, J. M.; Drumright, R. E. *J. Am. Chem. Soc*. **1992**, *114*, 1844.
(47) Padwa, A. *J. Am. Chem. Soc.* **1965**, *87*, 4205.
(48) Caldwell, R. A.; Majima, T.; Pac, C. *J. Am. Chem. Soc.* **1982**, *104*, 629.